Stability Control for Gob-Side Entry Retaining with Supercritical Retained Entry Width in Thick Coal Seam Longwall Mining

Zizheng Zhang [1,2,3,*] **, Xianyang Yu** [1]**, Hai Wu** [1] **and Min Deng** [4]

[1] Work Safety Key Lab on Prevention and Control of Gas and Roof Disasters for Southern Coal Mines, Hunan Provincial Key Laboratory of Safe Mining Techniques of Coal Mines, Hunan University of Science and Technology, Xiangtan 411201, China; 1010092@hnust.edu.cn (X.Y.); wuhai@hnust.edu.cn (H.W.)

[2] State Key Laboratory of Mining Disaster Prevention and Control Co-founded by Shandong Province and the Ministry of Science and Technology, Shandong University of Science and Technology, Qingdao 266590, China

[3] Key Laboratory of Safe and Effective Coal Mining, Ministry of Education, Anhui University of Science and Technology, Huainan 232001, China

[4] School of Resource & Environment and Safety Engineering, Hunan University of Science and Technology, Xiangtan 411201, China; dengmin@mail.hnust.edu.cn

* Correspondence: 1010096@hnust.edu.cn; Tel.: +86-151-9728-0267

check for updates

Abstract: Taking gob-side entry retaining with large mining height (GER-LMH) of the 4211 panel in the Liujiazhuang coal mine as the engineering background, a numerical simulation was conducted to study the surrounding rock deformation, stress, and plastic zone distribution of GER-LMH with respect to retained entry width. The concept of critical retained entry width of GER-LMH was proposed. In view of the deformation characteristics of surrounding rock, an innovative approach to determine the critical width of GER-LMH based on the cusp catastrophe theory was proposed. The cusp catastrophe functions were set up by approximate roadside backfill body rib convergence and roof subsidence series with respect to different retained entry widths. The critical retained entry width of GER-LMH was 4.0 m according to bifurcation set equations. Surrounding rock stability control principle and technique of GER-LMH was proposed, including "rib strengthening and roof control": road-in support with high pre-stress rockbolts and anchor cables, roadside backfill body construction technology with high-water quick consolidated filling materials and counter-pulled rockbolt, road-in reinforced support technology with hydraulic prop support and roof master. Field test and field monitoring results show that GER-LMH with supercritical retained entry width in the 4211 panel could meet the requirements for ventilation when the 4211 panel was retreating.

Keywords: large mining height; gob-side entry retaining; cusp catastrophe; critical retaining width; surrounding rock control

1. Introduction

Gob-side entry retaining (GER) was tested and applied in the UK, Germany, Poland, and Russia in the past few decades, while GER is widely applied in coal mining in China [1–7]. GER is a safe, green and efficient mining technology with advantages including reduced excavation rates, relief of the rapid movement of mining activities, improved coal recovery rates and settling of corner gas accumulation, lowered panel temperatures and optimized working environments [8–14]. However, GER would restrain the longwall panel advance speed. Figure 1 shows a typical section view of the GER schematic diagram. When the longwall panel advances a certain distance, the RBB will be constructed at a distance away from the active panel. The retained entry will be applied to the adjacent

longwall panel. Under this condition, the surrounding rock control of GER would be affected by overburden rock strata movements.

Currently, overburden rock strata movement of the longwall panel becomes more intense as the mining height increases, and this brings about great challenges to maintain the surrounding rock stability control for GER with large mining height (LMH). In China, the stability control techniques of GER with small sections in thin and mid-thick coal seams have been well optimized and improved [15]. Many experts and scholars have begun to study the GER-LMH and its field practice. Hua proposed that the roadside backfill body (RBB) support resistance increases as the mining height increases, and the support action to the retained entry from the solid coal rib should be considered [16]. Han proposed that the surrounding rock deformation is more sensitive to the reduction of the entry width when the entry height is more than 3.0 m based on a numerical simulation [17,18]. Xue studied the distribution characteristics of roof stress with respect to the mining height by theoretical calculation and numerical modeling methods [19]. Xue and Han obtained the deformation distribution characteristics of the entire section of the retained entry under the condition of 4.2 m large mining height, and proposed the GER-LMH control strategy [17,19]. All of the research results indicate that there is a critical retained entry width. When the retained entry width is less than the critical retained entry width, the GER surrounding rock deformation increases gently. When the retained entry width is more than the critical retained entry width, the GER surrounding rock deformation increases rapidly. However, few researchers have focused on the critical retained entry width with LMH and its surrounding rock control. Therefore, this paper attempts to analyze the critical retained entry width for GER-LMH in the Liujiazhuang coal mine based on cusp catastrophe theory, then proposes the adaptive surrounding rock stability control strategy of GER-LMH based on field tests, theoretical calculations, and numerical simulations.
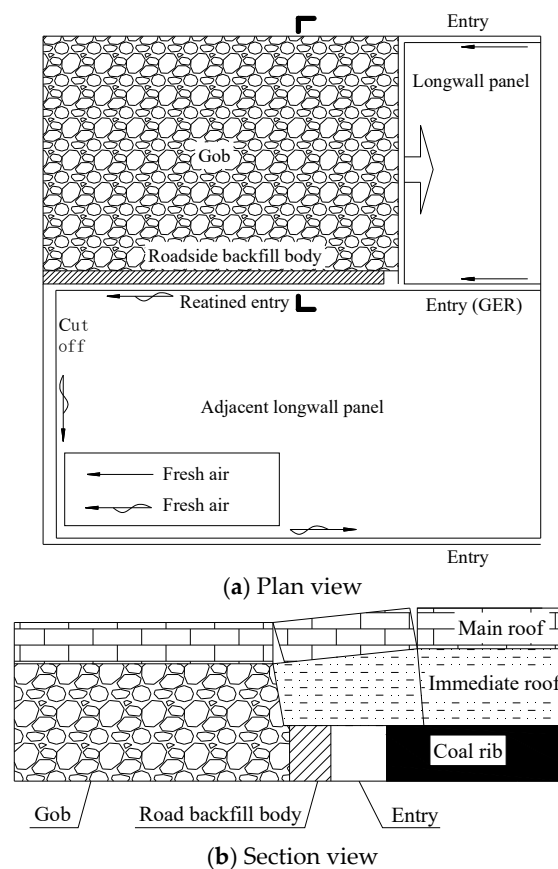

(**a**) Plan view

(**b**) Section view

Figure 1. View of the GER schematic diagram.

2. Mining and Geological Conditions

The current case study was based of the mining and geological conditions of the 4211 panel in the Liujiazhuang coal mine, Shanxi Province, China. The main #4 and #5 coal seams are 1.7 m and 1.8 m thick. The average thickness of the parting between the #4 and #5 coal seams is 0.5 m, and the parting is mined out coupled with the #4 and #5 coal seams. The average dip angle of the #4 and #5 coal seams is 4 degrees. The rock strata above the #4 and #5 coal seam consist of sandy mudstone (3.5 m thick), sandy mudstone and gritstone interbedding (6.3 m thick). Meanwhile, the floor strata below the #4 and #5 coal seams consist of sandy mudstone (4.5 m thick) and sandstone (7.0 m thick). The generalized stratigraphy of the 4211 panel is shown in Figure 2. The mining height of the 4211 panel is 4.0 m. The width of the 4211 panel is 200 m. The 4211 panel is developed by a three-entry system. All sections of the entries are 4.5 wide by 4.0 m high, which are excavated along the 5# coal seam floor (see Figure 3). The average overburden depth of the 4211 panel is 200 m. The coal pillar width between the 4211 haulage entry and 4211 air-return entry (GER) is 30 m.
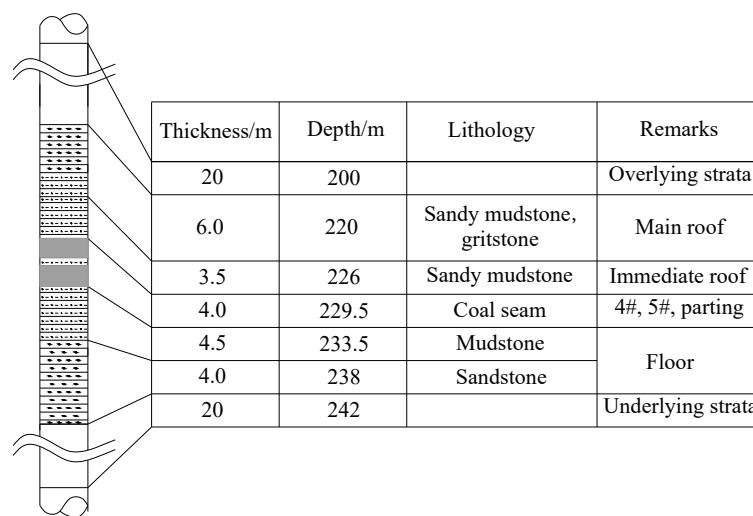

Thickness/m	Depth/m	Lithology	Remarks
20	200		Overlying strata
6.0	220	Sandy mudstone, gritstone	Main roof
3.5	226	Sandy mudstone	Immediate roof
4.0	229.5	Coal seam	4#, 5#, parting
4.5	233.5	Mudstone	Floor
4.0	238	Sandstone	
20	242		Underlying strata

Figure 2. Generalized stratigraphic column for the 4211 panel.

(**a**) Location site of the Liujiazhuang coal mine

Figure 3. *Cont.*

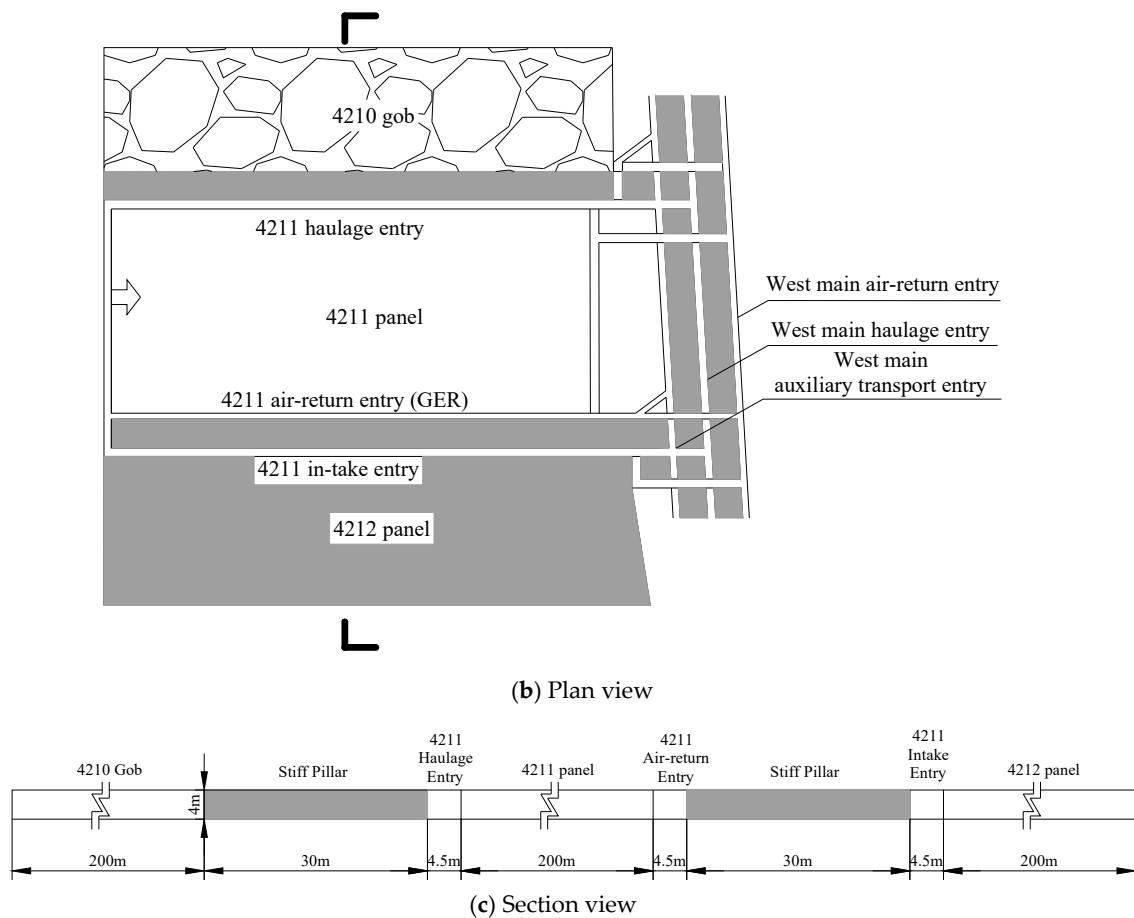(**b**) Plan view

(**c**) Section view

Figure 3. View of 4211 panel and location.

High-strength rockbolts and anchor cable were used in the roof support. The diameter and length of the roof rockbolts were 20 mm and 2.4 m, respectively. The rockbolt space of each row was 0.8 m. The space between two rows of the rockbolts along the entry length was 0.8 m. The diameter and length of the roof anchor cable were 17.8 mm and 6.3 m, respectively. The anchor cable space of each row was 1.6 m. The space between two rows of the anchor cable along the entry length was 2.4 m. A seven-hole "W" steel belt with 4.4 m long, 230 mm wide and 5 mm thick was used to connect the roof rockbolt. The metal mesh was made of #18 galvanized iron wire to cover the roof immediately. Meanwhile, rod bolt with 16 mm diametrical and 1.6 m long were employed in the coal rib support. The rod bolt space of each row was 0.8 m. The space between two rows of the rod bolts along the entry length was 0.8 m. A five-hole "W" steel belt with 3.8 m long, 230 mm wide and 5 mm thick was used to connect the rib rod bolt.

3. An Innovative Approach to Determine the Critical Width of GER-LMH

3.1. Cusp Catastrophe Theory for the Critical Width of GER-LMH

Cusp catastrophe theory has been widely used in mining engineering, geotechnical engineering and other underground mining activities [20–23]. The deformation process of GER surrounding rock can be regarded as the evolution process of deformation catastrophe with the increase of the retained entry width. Furthermore, the cusp catastrophe theory can be introduced to determine the critical width of GER-LMH. Zhang et al. indicated that the retained entry width has a significant impact on roof subsidence and RBB rib deformation [8,18,24]. Therefore, the critical width of GER-LMH can be obtained by fitting the mathematical function between roof subsidence (RBB rib deformation) and the retained entry width, establishing and computing the cusp catastrophe theory.

On the basis of the cusp catastrophe theory, the cusp catastrophe function $V(d)$ between roof subsidence (RBB rib deformation) and the retained entry width (d) can be expressed as follows:

$$V(d) = a_4 d^4 + a_3 d^3 + a_2 d^2 + a_1 d + a_0 \tag{1}$$

where, a_0, a_1, a_2, a_3, a_4 are polynomial fitting parameters.

As Equation (1) is not the standard form of the cusp catastrophe function, variable conversion is conducted to determine the standard cusp catastrophe function for the critical width of GER-LMH.

Defining $d = p - q$, $q = a_3/4a_4$, and substituting them into Equation (1), the rewritten cusp catastrophe function can be expressed as follows:

$$V = c_4 p^4 + c_2 p^2 + c_1 p + c_0 \tag{2}$$

$$\begin{bmatrix} c_0 \\ c_1 \\ c_2 \\ c_4 \end{bmatrix} = \begin{bmatrix} q^4 & -q^3 & q^2 & -q & 1 \\ -4q^3 & 3q^2 & -2q & 1 & 0 \\ 6q^2 & -3q & 1 & 0 & 0 \\ 1 & 0 & 0 & 0 & 0 \end{bmatrix} \begin{bmatrix} a_4 \\ a_3 \\ a_2 \\ a_1 \\ a_0 \end{bmatrix} \tag{3}$$

The standard cusp catastrophe function can be expressed as follows:

$$\frac{V}{c_4} = p^4 + mp^2 + np + C \tag{4}$$

Equation (4) is the steady state equation of the standard cusp catastrophe model for the critical width of GER-LMH. Phase space is a 3D space consisting of the state variable p and the variables m, n. m, n can be obtained by the following equation:

$$\left. \begin{array}{l} m = \frac{c_2}{c_4} = \frac{a_2}{a_4} - \frac{3a_3{}^2}{a_4{}^2} \\ n = \frac{c_1}{c_4} = \frac{a_1}{a_4} - \frac{a_2 a_3}{2a_4{}^2} + \frac{a_3{}^3}{8a_4{}^3} \end{array} \right\} \tag{5}$$

The critical point of the steady state function V is the solution of the equation. Hence, the balance surface Z can be obtained by defining the first derivative of Equation (4) to zero, i.e.,:

$$V' = 4p^3 + 2mp + n = 0 \tag{6}$$

Figure 4 shows the balance surface Z and bifurcation set. All points on the balance surface (p, m, n) are referred to as balance points of the steady state function V. The equation of singular points W can be obtained by the following equation:

$$V'' = 12p^2 + 2m = 0 \tag{7}$$

If the singularity points W is projected onto the control surface *m-n*, branch points Q can be obtained based on the critical state of the steady state equation as follows:

$$\Delta = 8m^3 + 27n^2 = 0 \tag{8}$$

When the control points (m, n) jump over a branch point Q, a discontinuous catastrophe will occur. The points located on the two branches of Q are singularity points of the system, i.e., catastrophe points.

Given natural effects and human activities, the GER system usually changes from a balanced state to an unstable state. When the retained entry width is in a critical condition, it is extremely sensitive to the increase of the retained entry width. A small increase of the retained entry width was likely to induce surrounding rock instability of GER, i.e., a catastrophe in GER.
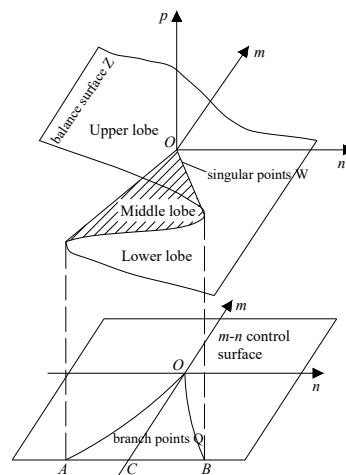
Figure 4. Balance surface Z and bifurcation set.

3.2. Implementation Procedure to Determine the Critical Retained Entry Width of GER-LMH Based on Cusp Catastrophe Theory

Implementation procedure to determine the critical retained entry width of GER-LMH based on the cusp catastrophe theory is as follows:

(1)   A 3D numerical model of GER-LMH is established, in which rock mechanical parameters are normally selected and determined;
(2)   3D numerical models with different retained entry width are established and calculated;
(3)   Roof subsidence and RBB deformation with respect to retained entry width can be obtained by setting monitoring points. Then cusp catastrophe function would be obtained by fitting the relationship between the retained entry width and roof subsidence (RBB deformation);
(4)   According to the cusp catastrophe criterion of the critical width of GER-LMH, the critical width of GER-LMH is determined by determining whether the roof subsidence and RBB deformation are mutated or not.

Calculation flow for the implementation procedure to determine the critical retained entry width of GER-LMH based on the cusp catastrophe theory is shown in Figure 5.
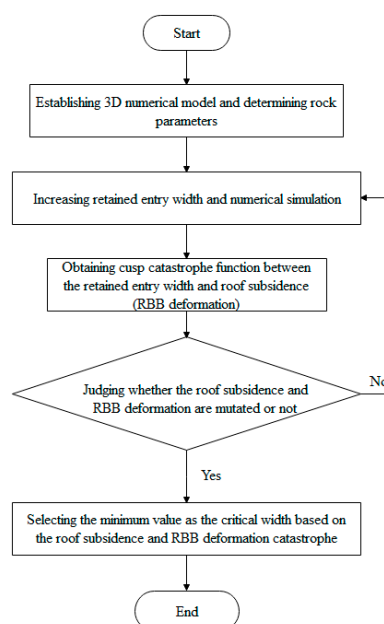

Figure 5. Calculation flow chart.

4. Relationship between Surrounding Rock Stability of GER-LMH and Retained Entry Width

4.1. 3D Numerical Model of GER-LMH

A 3D numerical model was constructed in FLAC3D software based on the 4211 panel mining and geological conditions in the Liujiazhuang coal mine. The model was consisted of part of the 4211 panel (100 m), part of the 4212 panel (100 m), and the entry system between them. The RBB width in the global model is 3.0 m. The dimensions of the model are 207.5 m × 100 m × 54 m (length ×width × height) along the x, y, and z axial direction, as shown in Figure 6. At the top of the model, a vertical load (vertical stress 5 MPa) is applied to simulate the overburden weight. According to the in-situ stress test results [25–27], the horizontal stress is equal to the vertical stress. The horizontal and bottom sides are roller constrained. The Mohr–Coulomb model is applied to simulate the rock strata including the RBB. On the basis of the laboratory results for the mechanical properties of rock and RBB, the parameters employed in the model have been determined. Moreover, some trial model tests have been carried out and the mechanical parameters are adjusted in reference to the in-situ measurement on the displacement [7,28–31]. The final rock strata property parameters in the numerical model are shown in Table 1. The modeling process is as follows: (i) calculating the initial state induced by the gravity; (ii) modeling the excavations of the 4211 air-return entry; (iii) retreating 4211 panel; (iv) modeling the retaining of the 4211 air-return entry with respect to retained entry width (2.5, 3.0, 3.2, 3.5, 3.8, 4.0, 4.5 and 5.0 m).
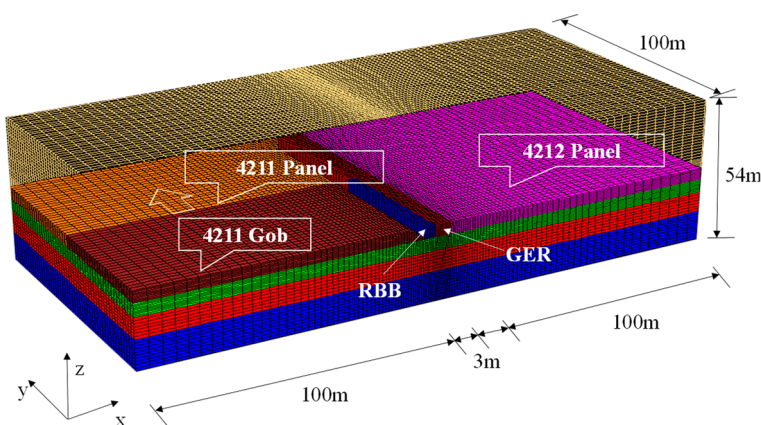

Figure 6. Numerical simulation model.

Table 1. Rock mechanics parameters.

Rock Strata	Bulk Modulus (GPa)	Shear Modulus (GPa)	Cohesion (MPa)	Friction Angle (°)	Tensile Strength (MPa)
Overlying rock strata	7.62	5.05	3.76	42	2.80
Main roof	9.35	6.13	3.92	42	3.88
Immediate roof	6.12	4.16	1.73	24	0.38
4# and 5# coal seam	4.94	2.43	1.50	24	0.20
Immediate floor	6.67	4.00	1.90	26	0.65
Main floor	9.35	6.13	2.92	40	1.23
Underlying rock strata	7.62	5.05	3.16	38	2.80
RBB	4.50	2.20	2.80	32	1.50

4.2. Surrounding Rock Stability of GER-LMH with Respect to Retained Entry Width

4.2.1. Surrounding Rock Deformation of GER-LMH with Respect to Retained Entry Width

The schematic diagram for GER deformation monitoring is shown in Figure 7. The deformation of the coal rib to the RBB rib can be obtained by measuring the horizontal distance between the A

pin and the B pin. The roof to floor deformation can be obtained by measuring the vertical distance between the C pin and D pin.
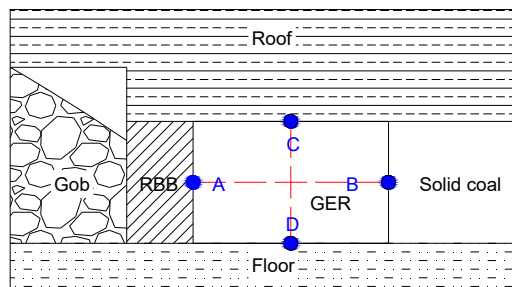

Figure 7. Schematic diagram for GER surrounding rock deformation monitoring.

Figure 8 shows the roof subsidence at the middle of the entry and RBB deformation at the middle of the RBB.
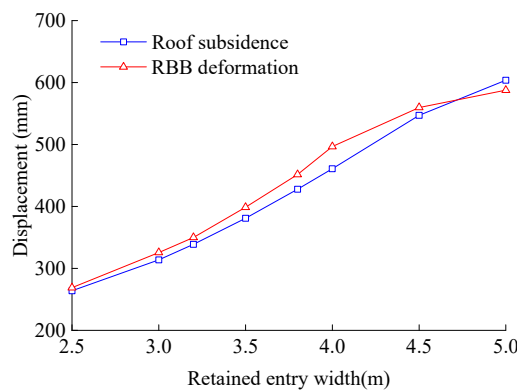

Figure 8. Relationship between the retained entry width and roof subsidence, RBB deformation.

It shows that the retained entry width has a significant impact on roof subsidence and RBB deformation; both the roof subsidence and RBB deformation increase as the retained entry width increases. Meanwhile, Figure 9 presents the increment of surrounding rock deformation for GER.
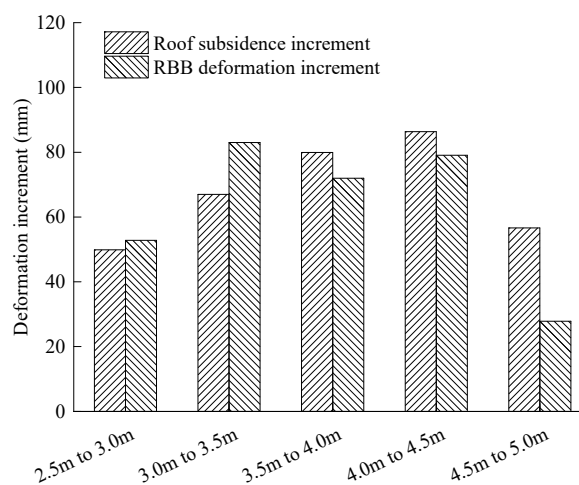

Figure 9. Increment of surrounding rock deformation for GER.

It shows that both the increment of roof subsidence and RBB deformation present a Λ-shaped distribution, i.e., there is a critical retained entry width. When the retained entry width is less than the critical value, both the increment of roof subsidence and RBB deformation increase. When the

retained entry width is more than the critical value, both the increment of roof subsidence and RBB deformation decrease.

4.2.2. Roof Plastic Zone Distribution of GER-LMH with Respect to Retained Entry Width

Numerical simulation results indicate that the retained entry width has a significant impact on roof plastic zone distribution rather than other parts of surrounding rock. Figure 10 shows the variation law of tensile failure area and tensile failure depth of roof.
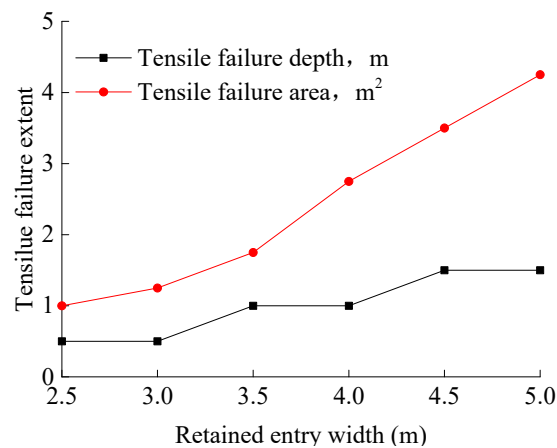

Figure 10. Effect of retained entry width on roof failure.

It can be seen that:

(1) When the retained entry width increases from 2.5 m to 4.5 m, the roof tensile failure depth increases from 0.5 m to 1.5 m while the roof tensile failure area increases from 1 m² to 3.5 m².
(2) There is a critical value of the retained entry width. When the retained entry width is no more than 4.0 m, the roof tensile failure depth is 1.0 m. When the retained entry width is more than 4.0 m, the roof tensile failure depth is 1.5 m.

4.2.3. Surrounding Rock Stress of GER-LMH with Respect to Retained Entry Width

The vertical stress distribution characteristics of the immediate roof are shown in Figure 11 by setting a measuring line on the immediate roof. The in-situ stress value at the depth of the measuring line was 5.57 MPa.
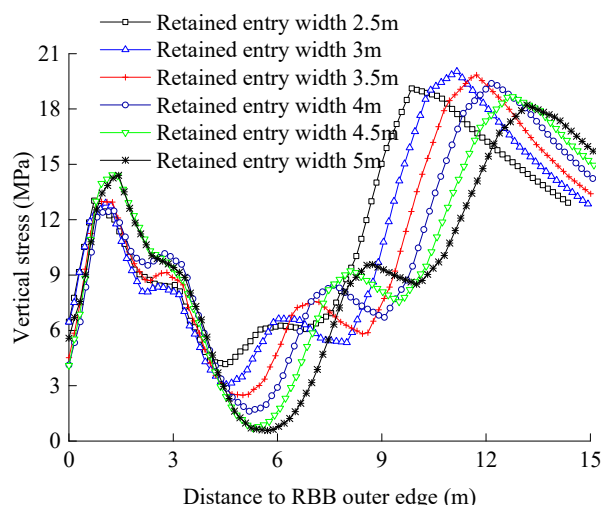

Figure 11. Vertical stress distribution of the immediate roof with respect to retained entry width.

It shows that:

(1) The vertical stress distribution exhibits apparent partition characteristics. Both the immediate roof above the RBB and above the solid coal rib are located in the zone of stress concentration, while the immediate roof above the retained entry is located in the zone of stress relief.

(2) The vertical stress distribution of the immediate roof forms a two peak distribution. The first peak occurs in the middle of the backfill area, and the second peak occurs above the solid coal. The second peak is larger than the first peak, and the location of the two peaks scarcely moves. The location of the second peak is about 5.2 m away from the solid coal rib.

Figure 12 shows the vertical stress of the immediate roof at the middle of the retained entry.
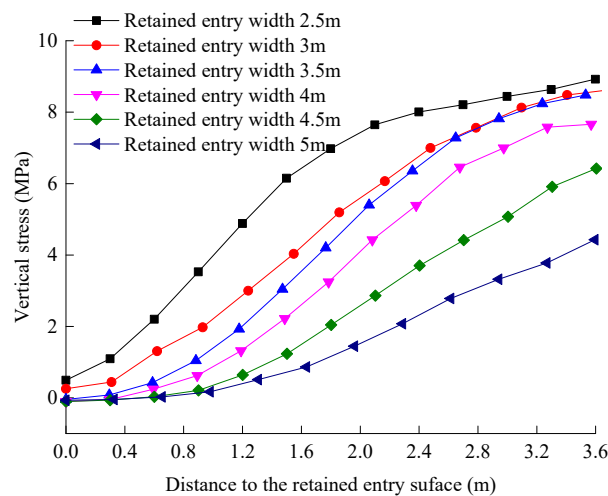

Figure 12. Vertical stress of the immediate roof at the middle of the retained entry.

It shows that:

(1) Vertical stress of the immediate roof above the entry increases as the distance away from the retained entry roof surface increases regardless of the retained entry width.

(2) Vertical stress of the immediate roof at the same depth decreases as the retained entry width increases. However, the stress relief zone increases for the surrounding rock at the same depth as the retained entry width increases. When the retained entry width is 3.5 m and 4.5 m, the depth of vertical stress below 4 MPa is 1.5 m and 3.5 m, respectively. Therefore, the larger the retained entry width, the more the vertical stress reduction and the greater the surrounding rock failure depth.

(3) Tensile stress occurs in the shallow part of the immediate roof. The range of tensile stress of the immediate roof increases as the retained entry width increases, and the range and degree of surrounding rock tensile failure increases.

5. Stability Control of Surrounding Rock for GER-LMH with Supercritical Width

5.1. Critical Width of GER-LMH

According to aforementioned calculation flow and numerical results, when RBB deformation is the independent variable, cusp catastrophe function between the retained entry width and RBB deformation can be obtained as follows (retained entry width is no more than 4.0 m):

$$V(d) = -11.054d^4 + 94.251d^3 - 187.07d^2 - 86.985d + 618.79$$

where, $\Delta = -8.669 \times 10^3 < 0$, i.e., a discontinuous catastrophe firstly occurs.

When roof subsidence is the independent variable, cusp catastrophe function between the retained entry width and roof subsidence can be obtained as follows (retained entry width is no more than 4.5 m):

$$V(d) = -1.4356d^4 + 12.863d^3 - 3.4416d^2 - 53.633d + 274.67$$

where, $\Delta = -1.23 \times 10^5 < 0$, i.e., a discontinuous catastrophe firstly occurs.

Therefore, when RBB deformation is the independent variable, the critical retained entry width is 4.0 m; when roof subsidence is the independent variable, the critical width is 4.5 m. The final critical retained entry width can be determined the smaller value synthetically, i.e., the critical retained entry width of GER with 4.0 m mining height is 4.0 m in the 4211 panel of the Liujiazhuang coal mine.

5.2. Stability Principle of Surrounding Rock for GER-LMH with Supercritical Retained Entry Width

The average mining height of the 4211 panel in the Liujiazhuang coal mine is 4.0 m. The retained entry width is 4.5 m more than the critical retained entry width while the RBB width is 3.0 m. Therefore, GER of the 4211 air-return entry is the GER with LMH and supercritical width. Stability principle of surrounding rock for MER-LMH with supercritical width was proposed including "rib strengthening and roof control".

"Rib strengthening" refers to high strength support by high strength and high pre-stress additional rockbolts to the solid coal rib and constructing the RBB with high-water quick consolidated filling materials and counter-pulled rockbolts:

(1) High strength and high pre-stress rockbolts were employed to reinforcement the solid coal rib by improving the support resistance to the roof, reducing the plastic zone depth and area of the solid coal rib, and transferring the concentrated stress to distant solid coal. Therefore, the rotation angle and subsidence of the overlying roof would decrease.

(2) High-water quick consolidated filling materials and counter-pulled rockbolts would be used to construct the RBB with strong bearing capacity and plastic deformation. Therefore, the roof above the RBB can be supported in time to recover the condition of three-dimensional pressure.

"Roof control" refers to reinforcement support by high pre-stress anchor cable to the roof above the retained entry and the RBB:

(1) High pre-stress anchor bolts were employed to enhance the support strength, improve the roof adhesion, and reduce the roof separation between the main roof and the immediate roof.

(2) Anchor cables were employed to support the roof above the RBB to restrain the tensile failure expansion for the shallow immediate roof. Meanwhile, the bending resistance of the roof was enhanced, the RBB support resistance was diminished, and the bearing capacity of the RBB was improved.

(3) Hydraulic props with high resistance were employed to support the roof to decrease the roof rotation and floor heave, which improved GER surrounding rock stability.

According to the numerical simulation results, Figure 13 shows the tensile failure distribution with respect to different support. It shows that the roof tensile failure depth around the RBB is greater than that around the solid coal rib. The maximum tensile failure depth is 3.5 m when there is no support to the entry. However, when the above mentioned support is employed, the tensile failure area and depth of the roof decreases evidently, especially the roof around the RBB. The maximum tensile failure depth of the roof is 1.0 m while that of the solid coal rib is 1.3 m, which is less than the rockbolt anchor depth. Hence, rockbolt support with anchor cables can reduce the tensile failure extent of the roof and the solid coal rib, and helps to stabilize the surrounding rock of GER-LMH with supercritical retained entry width.
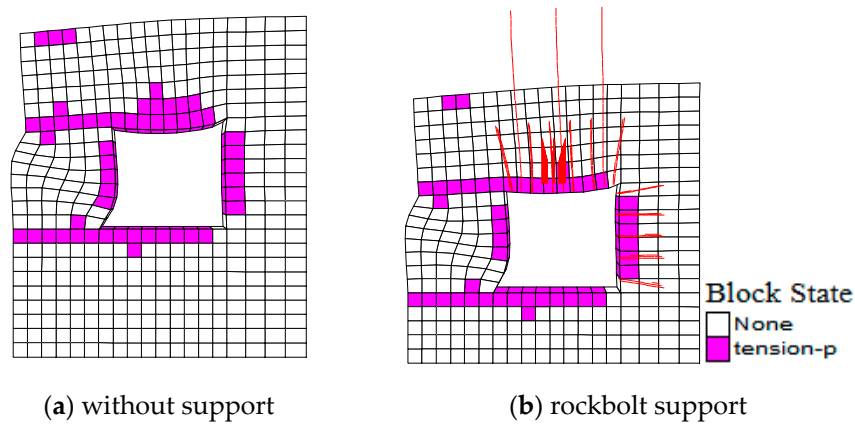
(**a**) without support (**b**) rockbolt support

Figure 13. Tensile failure distribution of GER surrounding rock.

5.3. Stability Technique of Surrounding Rock for GER-LMH with Supercritical Retained Entry Width

Both the rockbolt and anchor cable support are used to support the retained entry of 4211 panel. High-water quick consolidated filling materials and counter-pulled rockbolts are used to construct the RBB. The detailed support technique is as follows, and the designed support layout is shown in Figure 14.

Reinforcement support: A row of anchor cables with 18.9 mm diameter and 8.3 m length were employed to support the roof.

Roadside support: High-water quick consolidated filling materials with water-cement ratio 1.5:1 were employed to construct the RBB with 3.0 m width. Counter-pulled bolts with 22 mm diameter and 1.7 m length were employed to improve the bearing capacity of the RBB. The counter-pulled bolt space of each row was 0.8 m. The space between two rows of the counter-pulled bolts along the entry length was 0.8 m. Meanwhile, round steel ladder beam was welded with 16 mm diameter and 3.6 m length (see Figure 15).
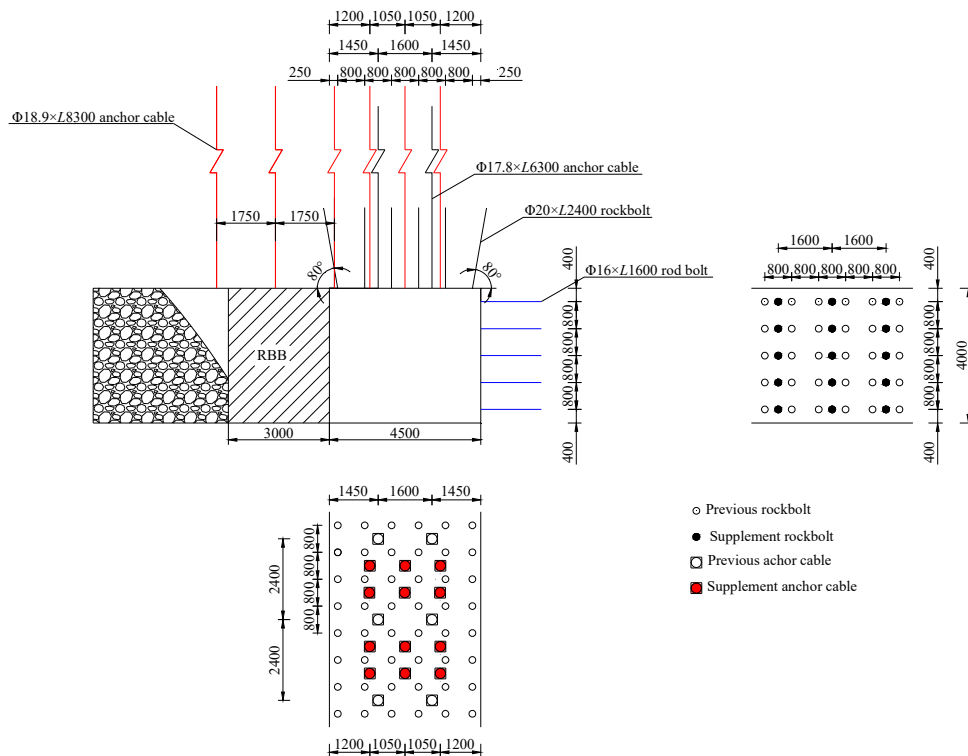

Figure 14. The 4211 air-return entry support layout for GER (units: mm).

Roof support above the RBB: A row of anchor cable with 18.9 mm diameter and 8.3 m length were employed to support the roof above the RBB. The anchor cable spacing of each row was 1.75 m. The space between two rows of the anchor cable along the entry length was 0.8 m.

Solid coal rib reinforcement support before the GER: A row of rockbolts with 20 mm diameter and 2.4 m long were employed to support the solid coal rib 100 m away from the active 4211 panel. The additional rockbolts would be located between the previous two rows of rod bolts.

Reinforcement support after GER: Hydraulic props with high resistance were employed to support the roof within the range of 120 m behind the active 4211 panel. A row of hydraulic props was retained with a space of 1.2 m and a distance off 0.45 m to the solid coal rib. The spacing between two rows of the props along the entry length was 1.0 m.
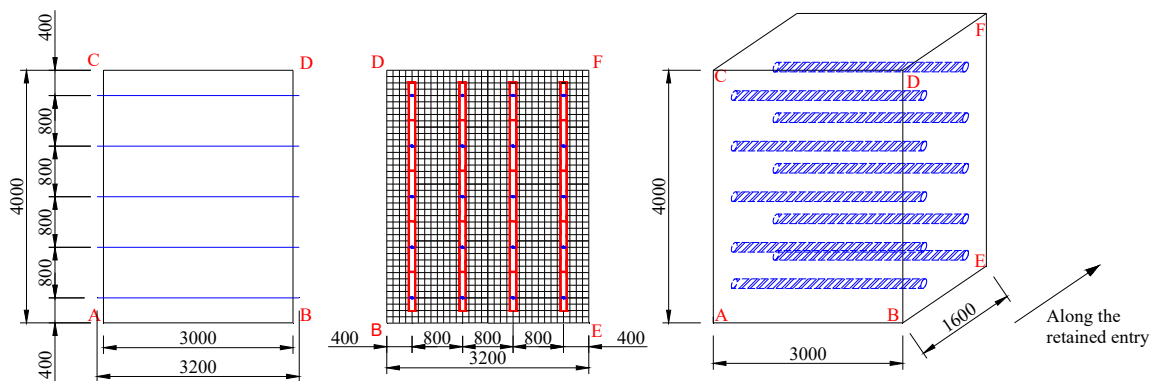

Figure 15. RBB for GER of the 4211 air-return entry (units: mm).

5.4. Stability Technique of Surrounding Rock for GER-LMH with Supercritical Retained Entry Width

To evaluate the performance of GER-LMH with supercritical retained entry width, field monitoring results of the GER-LMH with supercritical retained entry width during the period of 4211 panel mining are presented in Figure 16. The figure shows that when the active 4211 panel passed the monitoring site at a distance of 120 m, the roof to floor displacement and solid coal rib to RBB rib placement were about 440 mm and 634 mm, respectively.
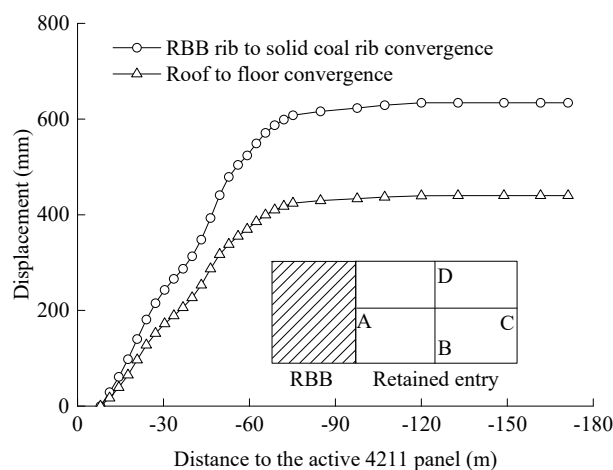

Figure 16. Monitoring results of the surrounding rock displacement.

Considering the minimum requirement of the retained entry section for ventilation and transportation, the section of the retained entry in the 4211 panel could meet the requirements. Field monitoring results showed that GER design of the 4211 panel in the Liujiazhuang coal mine was rational, and confirmed the feasibility of the GER-LMH with supercritical retained entry width.

6. Discussion

To calibrate the global numerical model, the calibrations of the global numerical model by comparing the outputs of the global numerical model with field monitoring results are essential.

In the field test, GER with supercritical retained entry width was conducted in the 4211 panel, and the construction speed of the retained entry is 1.8 m/day. Figure 17 shows the comparison between the field measured and numerical simulated displacement during the period of 4211 panel mining. The red solid line presents the numerical simulated roof to floor displacement and the blue solid line presents the numerical simulated RBB rib to coal rib displacement, while the filed monitoring GER surrounding rock displacement curves are shown by triangles and squares. Both the filed monitoring measured and numerical simulated GER surrounding rock displacement curves show a similar change trend. After a period, both the roof to floor displacement and RBB rib to coal rib displacement arrive a constant value.
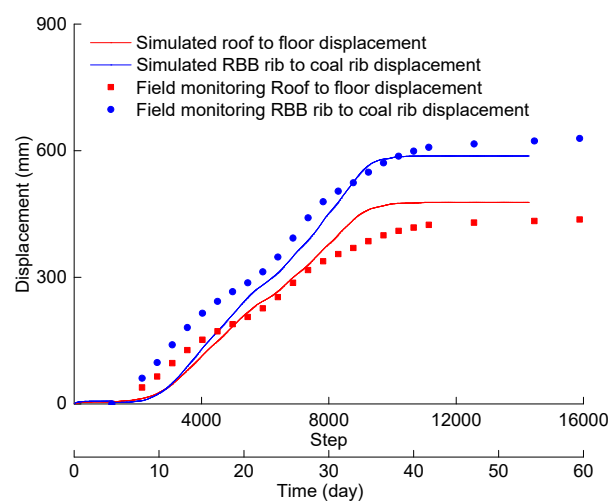

Figure 17. Comparison between the measured and simulated GER displacement.

7. Conclusions

(1) Numerical simulation results show that the retained entry width has a significant effect on surrounding rock stability of GER-LMH. Roof subsidence, RBB deformation of GER-LMH, roof tensile failure depth and tensile failure area increase as the retained entry width increases, which indicates a critical retained entry width.

(2) In the present study, an innovative approach to determine the critical width of GER-LMH based on cusp catastrophe theory has been proposed. The cusp catastrophe functions between roof subsidence (RBB rib deformation) and the retained entry width are established by increasing the retained entry width gradually. The critical retained entry width is determined according to the bifurcation set equation and cusp catastrophe functions. GER of the 4211 air-return entry with 4.5 m wide in the Liujiazhuang coal mine belongs to GER-LMH with supercritical width.

(3) The stability principle of surrounding rock for GER-LMH with supercritical width was proposed including "rib strengthening and roof control". Field tests and field monitoring results show that the GER-LMH with supercritical retained entry width in the 4211 panel with RBB 3.0 m wide and high-strength anchor cable-rockbolt support could meet the requirement for ventilation and transportation during the period of 4211 panel mining.

(4) The proposed approach based on cusp catastrophe theory provides criteria to judge how much the critical retained entry width should be. It also provides a new way for safe coal mine production under similar conditions.

References

1. Smart, B.G.D.; Haley, S.M. Further development of the roof strata tilt concept for pack design and the estimation of stress development in a caved waste. *Min. Sci. Technol.* **1987**, *5*, 121–130. [CrossRef]

2. Clark, C.A.; Newson, S.R. Review of monolithic pumped packing systems. *Min. Eng.* **1985**, *144*, 491–495.

3. Zhang, Z.Z.; Wang, W.J.; Li, S.Q.; Bai, J.B.; Hao, S.P.; Yu, X.Y. An innovative approach for gob-side entry retaining with thick and hard roof: A case study. *Teh. Vjesn. Tech. Gaz.* **2018**, *25*, 1028–1036.

4. Tan, Y.L.; Yu, F.H.; Ning, J.G.; Zhao, T.B. Design and construction of entry retaining wall along a gob side under hard roof stratum. *Int. J. Rock Mech. Min. Sci.* **2015**, *77*, 115–121. [CrossRef]

5. Luan, H.J.; Jiang, Y.J.; Zhou, L.J.; Lin, H.L. Stability control and quick retaining technology of gob-side entry: A case study. *Adv. Civ. Eng.* **2018**, *2018*, 1–13. [CrossRef]

6. Ning, J.G.; Wang, J.; Bu, T.T.; Hu, S.C.; Liu, X.S. An innovative support structure for gob-side entry retention in steep coal seam mining. *Minerals* **2017**, *7*, 75. [CrossRef]

7. Wang, F.; Jiang, B.Y.; Chen, S.J.; Ren, M.Z. Surface collapse control under thick unconsolidated layers by backfilling strip mining in coal mines. *Int. J. Rock Mech. Min. Sci.* **2019**, *113*, 268–277. [CrossRef]

8. Zhang, Z.Z.; Bai, J.B.; Chen, Y.; Yan, S. An innovative approach for gob-side entry retaining in highly gassy fully-mechanized longwall top-coal caving. *Int. J. Rock Mech. Min. Sci.* **2015**, *80*, 1–11. [CrossRef]

9. Gong, P.; Ma, Z.G.; Zhang, R.C.; Ni, X.Y.; Liu, F.; Huang, Z.M. Surrounding rock deformation mechanism and control technology for gob-side entry retaining with fully mechanized gangue backfilling mining: A case study. *Shock Vib.* **2017**, *2017*, 1–15. [CrossRef]

10. Jiang, L.S.; Kong, P.; Shu, J.; Fan, K.G. Numerical Analysis of Support Designs Based on a Case Study of a Longwall Entry. *Rock Mech. Rock Eng.* **2019**. [CrossRef]

11. Li, X.H.; Ju, M.H.; Yao, Q.L.; Zhou, J.; Chong, Z.H. Numerical investigation of the effect of the location of critical rock block fracture on crack evolution in a gob-side filling wall. *Rock Mech. Rock Eng.* **2015**, *49*, 1041–1058. [CrossRef]

12. Zhang, N.; Yuan, L.; Han, C.L.; Xue, J.H.; Kan, J.G. Stability and deformation of surrounding rock in pillarless gob-side entry retaining. *Saf. Sci.* **2012**, *50*, 593–599. [CrossRef]

13. Zhang, Z.Y.; Shimada, H.; Sasaoka, T.; Hamanaka, A. Stability control of retained goaf-side gateroad under different roof conditions in deep underground y type longwall mining. *Sustainability* **2017**, *9*, 1671. [CrossRef]

14. Yang, H.-Y.; Cao, S.-G.; Wang, S.-Q.; Fan, Y.-C.; Wang, S.; Chen, X.-Z. Adaptation assessment of gob-side entry retaining based on geological factors. *Eng. Geol.* **2016**, *209*, 143–151. [CrossRef]

15. Yan, S.; Liu, T.X.; Bai, J.B.; Wu, W.D. Key parameters of gob-side entry retaining in a gassy and thin coal seam with hard roof. *Processes* **2018**, *6*, 51. [CrossRef]

16. Hua, X.Z.; Ma, J.F.; Xu, T.J. Study on controlling mechanism of surrounding rocks of gob-side entry with combination of roadside reinforced cable supporting and roadway bolt supporting and its application. *Chin. J. Rock Mech. Eng.* **2005**, *24*, 2107–2118.

17. Han, C.L.; Zhang, N.; Qian, D.Y. Optimization analysis of span-depth ratio for roof safety control in gob-side entry retaining under large mining height. *J. Min. Saf. Eng.* **2013**, *30*, 348–354.

18. Han, C.L.; Zhang, N.; Xue, J.H.; Kan, J.G.; Zhao, Y.M. Multiple and long-term disturbance of gob-side entry retaining by grouped roof collapse and an innovative adaptive technology. *Rock Mech. Rock Eng.* **2018**. [CrossRef]

19. Xue, J.H.; Han, C.L. Strata behavior and control countermeasures for the gob-side entry retaining in the condition of large mining height. *J. Min. Saf. Eng.* **2012**, *29*, 466–473.

20. Li, C.D.; Tang, H.M.; Hu, X.L.; Li, D.M.; Hu, B. Landslide prediction based on wavelet analysis and cusp catastrophe. *J. Earth Sci.* **2009**, *20*, 971–977. [CrossRef]

21. Li, J.T.; Cao, P. Cusp catastrophe model of instability of pillar in asymmetric mining. *Appl. Math. Mech.* **2005**, *26*, 1100–1106.

22. Qin, S.Q.; Jiao, J.J.; Li, Z.G. Nonlinear evolutionary mechanisms of instability of plane-shear slope: Catastrophe, bifurcation, chaos and physical prediction. *Rock Mech. Rock Eng.* **2005**, *39*, 59–76. [CrossRef]

23. Wang, T.T.; Yan, X.Z.; Yang, H.L.; Yang, X.J. Stability analysis of the pillars between bedded salt cavern gas storages by cusp catastrophe model. *Sci. China Technol. Sci.* **2011**, *54*, 1615–1623. [CrossRef]

24. Chen, Y.; Bai, J.B.; Wang, X.Y.; Ma, S.Q.; Xu, Y.; Bi, T.F.; Yang, H.Q. Support technology research and application inside roadway of gob-side entry retaining. *J. China Coal Soc.* **2012**, *37*, 903–910.

25. Kang, H.P.; Yi, B.D.; Gao, F.Q.; Lv, H.W. Database and characteristics of underground in-situ stress distribution in Chinese coal mines. *J. China Coal Soc.* **2019**, *44*, 23–33. [CrossRef]

26. Kang, H.P.; Si, L.P.; Zhang, X. Characteristics of underground in-situ stress distribution in shallow coal mines and its applications. *J. China Coal Soc.* **2016**, *41*, 1332–1340. [CrossRef]

27. Kang, H.P.; Lin, J.; Yan, L.X.; Zhang, X.; Wu, Y.Z.; Si, L.P. Study on characteristics of underground in-situ stress distribution in Shanxi coal mining fields. *Chin. J. Geophys.* **2009**, *52*, 1782–1792. [CrossRef]

28. Mohammad, N.; Reddish, D.; Stace, L. The relation between in situ and laboratory rock properties used in numerical modelling. *Int. J. Rock Mech. Min. Sci.* **1997**, *34*, 289–297. [CrossRef]

29. Shen, W.L.; Bai, J.B.; Li, W.F.; Wang, X.Y. Prediction of relative displacement for entry roof with weak plane under the effect of mining abutment stress. *Tunn. Undergr. Space Technol.* **2018**, *71*, 309–317. [CrossRef]

30. Wang, X.Y.; Wang, R.F.; Zhang, Z.Z. Numerical analysis method of shear properties of infilled joints under constant normal stiffness condition. *Adv. Civ. Eng.* **2018**, *2018*, 1–13. [CrossRef]

31. Wu, Q.H.; Weng, L.; Zhao, Y.L.; Guo, B.H.; Luo, T. On the tensile mechanical characteristics of fine-grained granite after heating/cooling treatments with different cooling rates. *Eng. Geol.* **2019**, *253*, 94–110. [CrossRef]